

Modeling of Velocity-dependent Frictional Resistance of a Capsule Robot Inside an Intestine

Cheng Zhang · Hao Liu · Renjia Tan ·
Hongyi Li

Received: 6 March 2012 / Accepted: 9 May 2012 / Published online: 2 June 2012
© Springer Science+Business Media, LLC 2012

Abstract A model is first built for predicting the velocity-dependent frictional resistance of a capsule robot that moves inside the intestine in the paper. The capsule robot plays a more and more important role in checking diseases in the intestine. This study aims to optimize the locomotion mechanism and the control strategy of the capsule robot. The model consists of three parts: environmental resistance, viscous friction, and Coulomb friction. Environmental resistance is induced by the stress due to the viscoelastic deformation of the intestinal wall. Viscous friction is analyzed according to the apparent viscosity of intestinal mucus. Coulomb friction is a product of the local contact pressure and the Coulomb friction coefficient. In order to analyze the effects of the intestinal deformation, a five-element model is used to describe the stress relaxation of the intestinal material. Experimental investigation is used to identify the model parameters with homemade physical simulation measurement system and fixtures. Finally, the model's validity is verified by experimental results. It is shown that the model predicting results can fit the experimental results well when the moving velocity of the capsule is lower than 20 mm/s. The R^2 of these two sets of data is 0.8769. But at a higher velocity, there are significant differences between the two results and the R^2 declines to 0.1666. The friction model is expected to be useful in the development of the medical equipment in the intestine and the study of biomechanics of the intestine.

Keywords Friction model · Velocity-dependent · Intestine · Viscoelasticity

1 Introduction

Recently, the incidence of diseases in intestine has been increasing annually in the worldwide. As a method of minimally invasive inspection in intestine, capsule endoscopy (CE) is of great advantage comparing with the traditional endoscope. CE has become the gold standard for the diagnosis of most diseases of the intestine [1, 2].

However, the passive feature of CE makes it beyond control in the intestine. During an 8-h inspection, problems of missed diagnosis and ileus are possible [3]. To improve the situation, active CE equipment with a self-actuation mechanism, which is called capsule robot, is currently under development in several laboratories [4–9]. Before a practicable solution can be devised, the frictional resistance of the intestine needs to be researched.

Many developers work on the biomechanical and tribological properties of the intestine. Hoeg et al. [10] studied the tissue distention of the intestine when a robotic endoscope moved through. An analytical model and an experimental model were developed to predict the tissue behavior in response to loading. Huang and co-workers [11] analyzed frictional resistance changes under the influence of the diameter, length and material of the capsule robot by means of experimental investigation. Kim and co-workers [12] investigated the frictional resistance characteristics of a capsule inside the intestine of a pig with respect to various capsule shapes using a specially designed tribological tester. Then, the group found that the variation of resistance was correlated with the

C. Zhang · H. Liu (✉) · R. Tan · H. Li
State Key Laboratory of Robotics, Shenyang Institute
of Automation (SIA), Shenyang 110016, China
e-mail: liuhao@sia.cn

C. Zhang · R. Tan
Graduate University of the Chinese Academy of Sciences,
Beijing 100049, China

viscoelasticity of the intestine. A five-element model is used to describe the viscoelastic property of the intestinal stress relaxation [13]. Furthermore, the group first developed an analytical model for the frictional resistance prediction, which was verified by finite element analyses [14]. Wang and Meng [15] and Wang and Yan [16] studied frictional resistance changes under the influence of the shape, diameter and velocity of the capsule robot as well. Most of the researchers focus on the effects on contour parameters of the capsule robot. However, we find that the velocity of the capsule robot is important to frictional resistance.

The capsulbot with “internal force–static friction” driving principle is first developed by our group [17]. It can move at 32 mm/s on the hard surface. But inside the intestine, the velocity decreases to 1–2 mm/s. A main reason is that the frictional resistance inside the intestine is ignored in the setting of the driving parameters, especially the velocity-dependent frictional resistance. In order to increase the movement efficiency of the capsulbot, we got a qualitative relationship between velocity and friction resistance in our previous work. But a quantitative model is necessary in practice. The model is expected to make a contribution to the development of the medical equipment in the intestine in the future.

In the paper, an analytical velocity-dependent friction model is developed, which consists of Coulomb friction, viscous friction, and environmental resistance induced by the stress due to the viscoelastic deformation of the intestinal wall. A physical simulation measurement system is built to measure the Coulomb friction coefficient and the viscoelasticity of the intestine. The experimental results are used to identify the parameters of the model and verify the model’s validity.

The following sections describe the details of the model development.

2 Model Building for Velocity-dependent Frictional Resistance

When a capsule moves inside the intestine, various forces are applied to the capsule and the intestine. Velocity has a great effect on these forces. As a result, the velocity-dependent frictional resistance of the capsule $f(v)$ can be expressed as

$$f(v) = f_e + f_v + f_c \quad (1)$$

where f_e is the environmental resistance, f_v is the viscous friction, and f_c is the Coulomb friction.

Environmental resistance is the frictional resistance induced by the stress due to the viscoelastic deformation of the intestinal wall. Viscous friction of the model is the

resistance caused by the rheological properties of the intestinal mucus. Coulomb friction is a product of the local contact pressure and the Coulomb friction coefficient. Next, environmental resistance, viscous friction, and Coulomb friction will be analyzed, respectively.

2.1 Intestinal Deformation and Environmental Resistance Analyses

2.1.1 Principle of Environmental Resistance and Assumptions

The deformation of the intestinal wall induced by the capsule needs to be understood in order to analyze the stress and normal force applied to the capsule moving inside the intestine. Figure 1 illustrates the deformation of the intestine when a capsule is inserted. The capsule is a cylinder with two hemispheres on both ends. As the front of the capsule is a hemisphere, the intestinal wall applies a skew resistance on its contact surface. The horizontal component of the skew resistance is f_e . For further development of the model, the following assumptions are made.

- (1) The material of the intestine is incompressible.
- (2) The intestine consists of an isotropic material and deforms symmetrically towards its radial direction.
- (3) The deformation of the intestine is the same as the external shape of the contact surface of the capsule.

Based on the assumptions above, the deformation could be derived using the contact geometry between the intestine and the capsule.

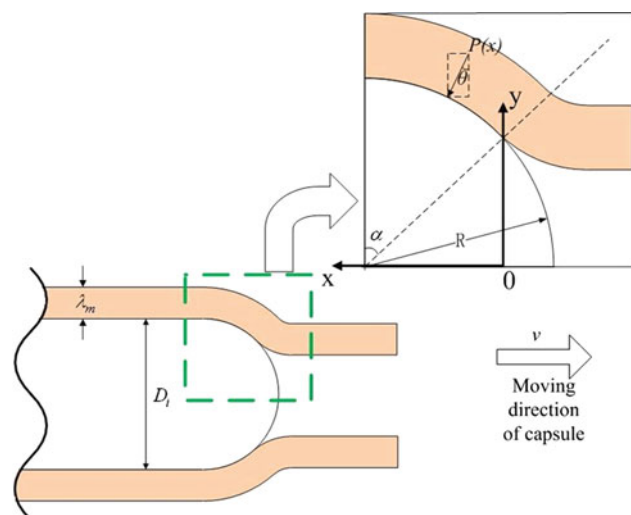


Fig. 1 Schematic diagram of the intestine deformation after the insertion of a capsule

2.1.2 Formula Derivation of Intestinal Deformation and Environmental Resistance

The skew resistance is mainly caused by the hoop stress of the intestine, which is shown in Fig. 2. The relationship between the pressure $P(x)$ and the hoop stress $\tau_\theta(x)$ can be expressed as [18]

$$\tau_\theta(x) = \frac{P(x)D_i(x)}{2\lambda_m} \tag{2}$$

where $D_i(x)$ is the inner diameter of the intestine at position x and λ_m is the mean value of the intestinal wall thickness.

A five-element model has been used to describe the hoop stress of the intestine of a pig, which consists of three springs and two dampers (see Fig. 3). An equation that shows the relationship between stress and strain with respect to time is obtained from the experimental results of a stress relaxation test [19]

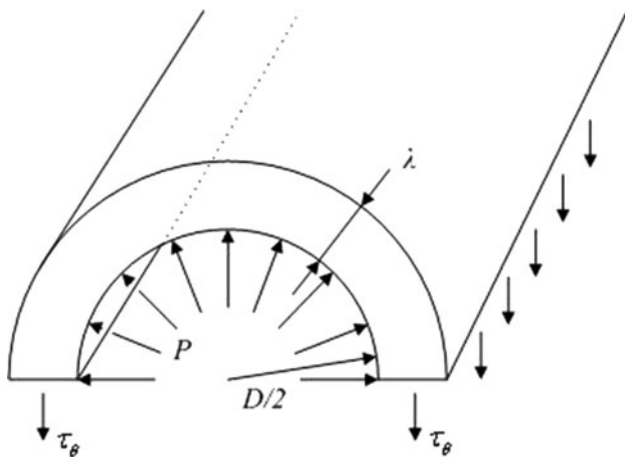


Fig. 2 Hoop stress of the intestine

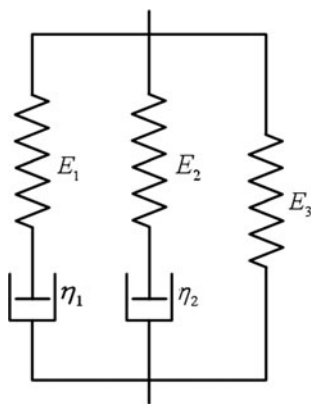


Fig. 3 Five-element model

$$\tau_\theta(t) = \varepsilon(t) \left[E_1 e^{\left(-\frac{E_1 t}{\eta_1}\right)} + E_2 e^{\left(-\frac{E_2 t}{\eta_2}\right)} + E_3 \right] \tag{3}$$

where E_1 , E_2 , and E_3 indicate the moduli of elasticity of springs, while η_1 and η_2 are the viscosity coefficients of the dampers. $\varepsilon(t)$, and $\tau_\theta(t)$ are the strain and stress applied to the intestine, respectively at the time t . When the capsule moves at a constant speed v , Eq. (3) can be written as a function of the position x

$$\tau_\theta(x) = \varepsilon(x) \left[E_1 e^{\left(-\frac{E_1 x}{\eta_1 v}\right)} + E_2 e^{\left(-\frac{E_2 x}{\eta_2 v}\right)} + E_3 \right]. \tag{4}$$

The initial mean diameter of the intestinal inwall approximately equals

$$D_{i0} = 2R \cos \alpha \tag{5}$$

where R is the radius of the hemisphere and α is the angle corresponding with the contact surface. The hoop strain with respect to position is defined as

$$\varepsilon(x) = \frac{D_i(x) - D_{i0}}{D_{i0}}. \tag{6}$$

Therefore, the contact pressure is

$$P(x) = \frac{\varepsilon(x) \left[E_1 e^{\left(-\frac{E_1 x}{\eta_1 v}\right)} + E_2 e^{\left(-\frac{E_2 x}{\eta_2 v}\right)} + E_3 \right] 2\lambda_m}{D_i(x)}. \tag{7}$$

The contact surface area is defined as

$$S = 2\pi R^2 \sin \alpha. \tag{8}$$

Then the environmental resistance induced by the stress is

$$f_e = P(x)S \cdot \sin(\theta). \tag{9}$$

where θ is slant angle of the skew resistance. The environmental resistance f_e varies with the velocity of the capsule according to Eq. (7).

2.2 Viscous Friction Analyses

There is lots of mucus on the intestinal inwall because of its own physiological structure. The capsule robot is in complete lubrication condition in the whole moving process approximately. Viscous friction is related to the relative velocity. It can be calculated from the empirical Eq. (10),

$$f_v = \delta v \tag{10}$$

where δ is apparent viscosity coefficient.

The intestinal mucus is a kind of non-newtonian fluid. Its apparent viscosity decreases with increasing shear rate. When the shear rate is high enough, the apparent viscosity

of the intestinal mucus becomes a constant. The apparent viscosity coefficient can be expressed as [20]

$$\delta = 11.24 \left(\frac{v}{d} \right)^{-0.7552} + 0.1148 \quad (11)$$

where d is the mean value of the intestinal mucus thickness. According to experimental results, the value of d is $30 \mu\text{m}$ [21].

2.3 Coulomb Friction Analyses

Coulomb friction is decided by the local contact pressure and the friction coefficient

$$f_c = \mu N \quad (12)$$

where f_c is Coulomb friction, μ is the Coulomb friction coefficient, and N is the local contact pressure.

The Coulomb friction coefficient is influenced by the surface texture of the intestine, especially the intestinal villi. The value of μ can be calculated from the experimental results. The local contact pressure consists of the normal force and the radial pressure. The normal force is decided by the weight of the capsule. The radial pressure is caused by the hoop stress of the intestine. It is the vertical component of the skew resistance on the hemisphere, which is expressed as

$$N = P(x)S \cdot \cos(\theta) \quad (13)$$

especially at the side of the capsule, $\theta = 0$.

Several parameters should be confirmed to complete the model. Experimental results are the main basis of parameter identification.

3 Experimental Design and Model Parameter Identification

3.1 Physical Simulation Measurement System

The physical simulation measurement system consists of two parts: drive unit and data acquisition (DAQ) unit (see Fig. 4).

The main part of the drive unit is NLA-7SL series coreless linear motor, which is produced by NIKKI DENSO. The encoder is RGH22X-lum resolution, which is produced by RENISHAW. The accuracy of positioning of the system can reach $1 \mu\text{m}$. The rotor of the linear motor is combined with a support, on which a single freedom-degree micro force sensor is fixed, whose accuracy is 5 mN . The right side of the drive unit is load platform.

PCI 6229 DAQ card produced by NI is used to acquire the voltage signal of encoder and micro force sensor. Then the signal is transmitted to computer for saving and analysis.

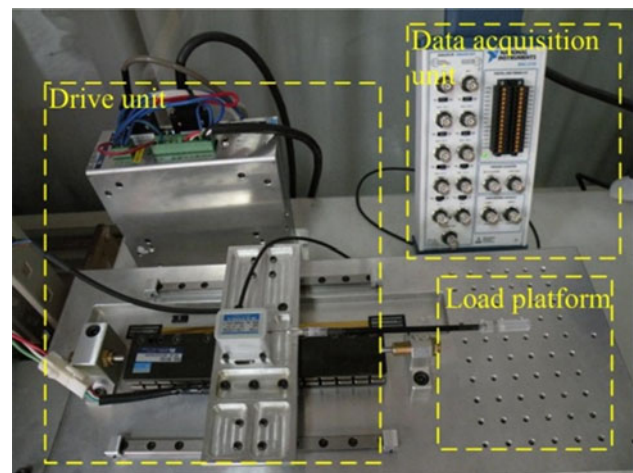


Fig. 4 Physical simulation measurement system

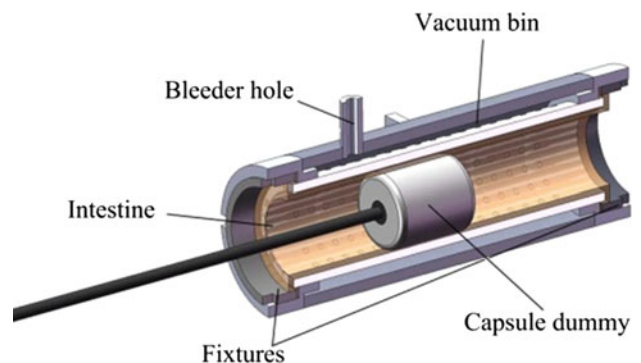


Fig. 5 3D model of negative pressure suction device

3.2 Shear Stress Relaxation Test of Intestine

Fresh intestine of a pig is used in the experiment. The intestine sample is stored in Tyrode with oxygen ventilating. A length of intestine is placed in negative pressure suction device (see Fig. 5). Both ends of the intestine are fixed. The air in vacuum bin is extracted from bleeder hole with a syringe. Then the intestinal wall is absorbed by the device and mandatorily expanded. The device is fixed on the load platform and a capsule dummy is inserted into the intestine that is fully expanded. The capsule dummy is a cylinder whose diameter is 12.9 mm and height is 15.2 mm . It is dragged by the drive unit to make a shear stress relaxation test.

There are asperities on the surface of the capsule dummy. These asperities will ensure that there is no relative slippage between the dummy and the intestine. The experimental shear strains, which are the ratios of the intestinal elongation and the intestinal wall thickness, are 50, 100, 150, and 200 %, respectively. The shear stress curves with different strains are obtained by means of

curve fitting, and then the parameters of the five-element model are confirmed (see Table 1) [19].

The moduli of elasticity and the viscosity coefficients of the five-element model are not constant, but vary with shear strains from Table 1. Therefore, the relationships between the parameters of the five-element model and the shear strains are shown in Eq. (14)

$$\begin{aligned}
 E_1 &= -0.1617\varepsilon^2 - 0.3175\varepsilon + 3.348 \\
 E_2 &= 0.1729\varepsilon^2 - 1.078\varepsilon + 2.078 \\
 E_3 &= 0.1653\varepsilon^2 - 0.9792\varepsilon + 1.877 \\
 \eta_1 &= -0.01386\varepsilon^2 + 0.03667\varepsilon + 0.0442 \\
 \eta_2 &= 0.0185\varepsilon^2 - 0.2205\varepsilon + 0.6971.
 \end{aligned}
 \tag{14}$$

3.3 Model Parameter Identification

The dimensions of the capsule using in the model is shown in Fig. 6. The mean value of the intestinal wall thickness λ_m is 2.5 mm. The angle corresponding with the contact surface α is 60° .

The curves of skew resistances that vary with the velocity are shown in Fig. 7. The intestine expands with x increasing from zero as shown in Fig. 2. The maximal skew resistance appears at a point on the hemisphere, but not at the maximum hoop strain point, because the hoop strain rate affects the relationship between the hoop stress and hoop strain. As time goes on, the skew resistances decrease because of the stress relaxation of the intestine. The horizontal component of the skew resistance is the environmental resistance and the vertical component is radial pressure. When $R \sin \alpha \leq x < R \sin \alpha + 20$, the

Table 1 Parameters of five-element model

Shear strain (%)	E_1 (kPa)	E_2 (kPa)	E_3 (kPa)	η_1 (kPa)	η_2 (kPa)
50	2.926	1.539	1.422	0.053	0.561
100	3.159	1.216	1.064	0.078	0.555
150	2.781	0.948	0.812	0.067	0.393
200	1.726	0.484	0.541	0.060	0.320

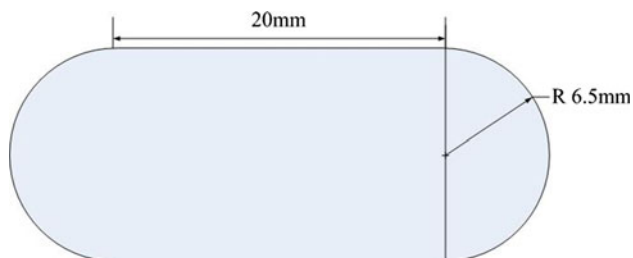


Fig. 6 The dimensions of the capsule

radial pressure is regarded as the skew resistance at $x = R \sin \alpha$. When $x \geq R \sin \alpha + 20$, the skew resistance is ignored, because the intestine needs time to restore tight.

The negative pressure suction device is used to measure Coulomb friction as well. The inside diameter of the intestine is mandatorily expanded to 13 mm in the negative pressure suction device. A capsule with a smooth surface whose diameter is 13 mm and mass is 50.1 g is dragged by the drive unit at the speed of 0.5 mm/s. Then Coulomb friction is shown in Fig. 8, where Savitzky–Golay filter is used to filter the noise of the primary data. The mean value of Coulomb friction is $f_c = 40.07$ mN. The Coulomb friction coefficient is $\mu = 0.082$ by calculation.

Environmental resistance, viscous friction, Coulomb friction and the summation of them are shown in Fig. 9. Environmental resistance is affected by the velocity greatly and occupies major share in frictional resistance. Viscous

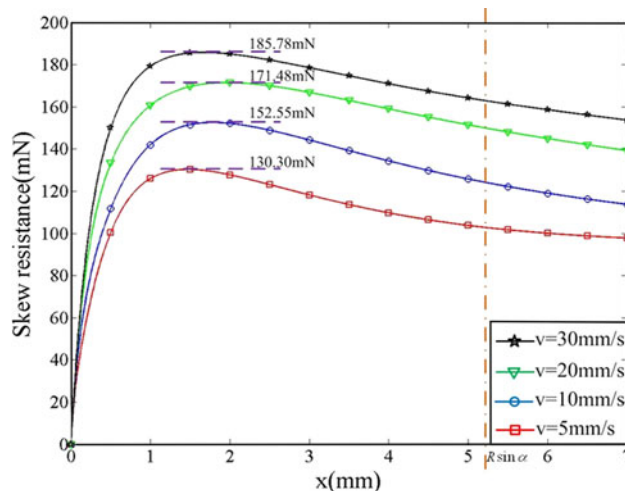


Fig. 7 Skew resistances varying with the velocity

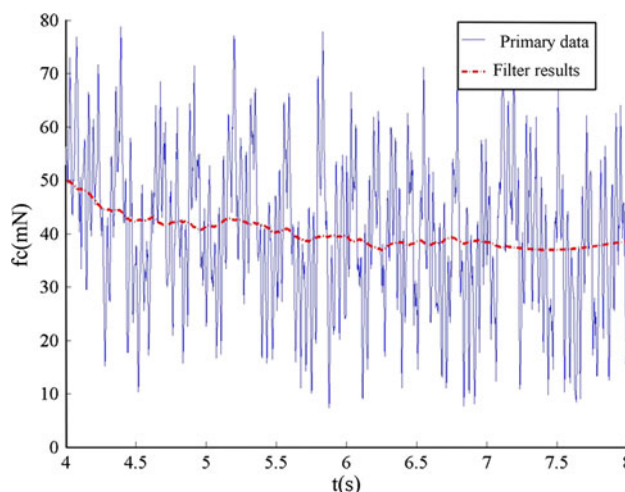


Fig. 8 Coulomb friction of the capsule at 0.5 mm/s

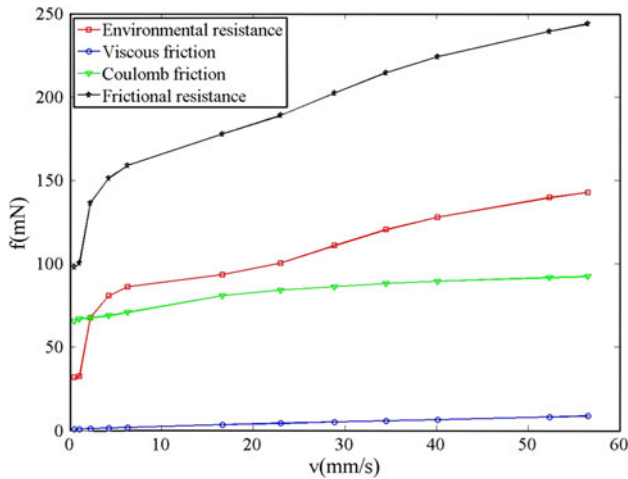


Fig. 9 Velocity-dependent frictional resistance of the capsule

friction is also affected by the velocity, but in a small proportion. Coulomb friction has little relationship with the velocity. In conclusion, the velocity-dependent frictional resistance of the capsule is the summation of environmental resistance, viscous friction and Coulomb friction. It increases with velocity logarithmically.

4 Model Validation and Discussion

The validity of the velocity-dependent frictional model should be verified by experiment. The physical simulation measurement system and another fixture are used to design the experiment. Flexible polyurethane foam (PUF) is chosen as a basement, which is fixed on the load platform. One side of the intestine specimen and the mesentery are fixed on the basement. The capsule dummy is inserted into the intestine by the drive unit at different velocity (see Fig. 10).

The relationship between the frictional resistance and the velocity is obtained from the experiment [22]. The comparison between the experimental results and the model predicted results is shown in Fig. 11.

R^2 that is the square of the correlation between two sets of data is used to measure how successful the fit is in explaining the variation of the data. The formula of R^2 is

$$R^2 = \frac{\sum_{i=1}^n (f_1(i) - \bar{f}_1)^2}{\sum_{i=1}^n (f_2(i) - \bar{f}_1)^2} \quad (15)$$

where f_1 is the model predicted results, f_2 is the experimental results, and \bar{f}_1 is the mean value of f_1 . When the velocity is lower than 20 mm/s, the model predicted results approximately coincide with the experimental results. The R^2 of these two sets of data is 0.8769. But there are significant differences between the two results and the R^2 declines to 0.1666 at a higher velocity. This result is identical with the conclusion in Ref. [22].

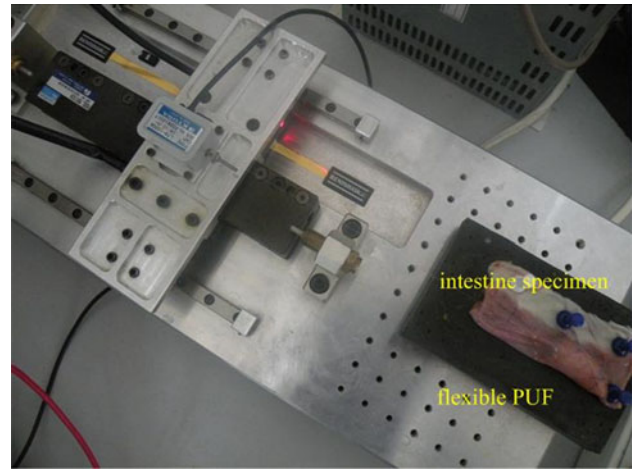


Fig. 10 Device of the model validation experiment

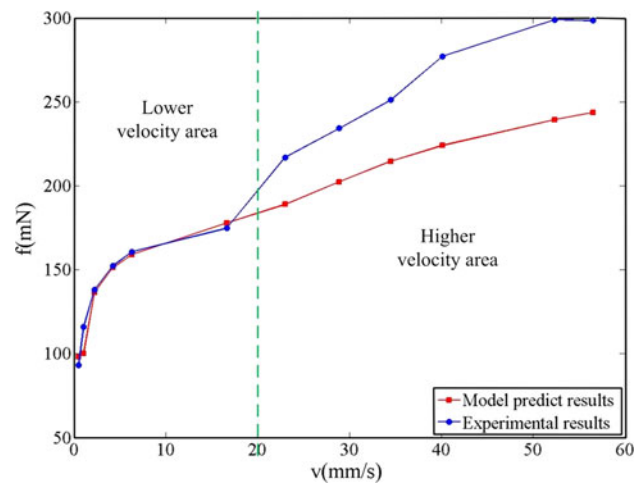


Fig. 11 Comparison between the experimental results and the model predicted results

The differences between the truth and the model prediction may be caused by several facts. First, the assumption (3) in Sect. 2.1.2 is false at a higher velocity because of a bigger inertia caused by higher velocity, which results in the model error. Second, when the capsule moves at a higher velocity, the five-element model cannot describe the viscoelasticity of the intestinal material completely. The hyperelasticity of the intestinal muscular layer may play a more important role in the intestinal deformation at a higher velocity [23].

There are a number of questions need to be studied in the model, such as whether the velocity boundary between the lower velocity area and the higher velocity area is an accurate value and whether the velocity boundary is relative to the intestinal material characteristics. A more accurate material model of intestine is necessary for the friction model as well. Further study is needed to perfect the model.

The model has been used in the movement parameters optimization of the capsuobot. Now the capsuobot can move at 7–10 mm/s inside the intestine. The result shows that the velocity-dependent frictional model contributes to the design of the capsule robot.

5 Conclusion

For the purpose of optimizing the locomotion mechanism and the control strategy of the capsule robot, a model aiming to analyze the velocity-dependent frictional resistance is first built, when the capsule robot moves inside the intestine. The model is developed by considering Coulomb friction, viscous friction, and environmental resistance. In order to investigate the hoop stress of the intestine applied to the capsule and to verify the model, experimental investigation is used with the homemade physical simulation measurement system and fixtures. From the comparison between the experimental results and the model predicted results, the R^2 is 0.8769 at a lower velocity, but is 0.1666 at a higher velocity. The intestinal biodiversity and the geometrical constraints on the deformation have an effect on the accuracy of the model, and above all, the viscoelasticity of the intestine at a higher velocity is different from that at a lower velocity. The hyperelasticity of the intestinal muscular layer may play a more important role in the intestinal deformation at a higher velocity. Further study is needed to perfect the model. The results of this study are expected to contribute to the development of the medical equipment in the intestine and the study of biomechanics of the intestine.

Acknowledgments This study was supported by the National Technology R&D Program of China, under the Contract Number 2012BAI14B03 and Project 61105099 supported by National Natural Science Foundation of China.

References

- Munoz-Navas, M.: Capsule endoscopy. *World J. Gastroenterol.* **15**(13), 1584–1586 (2009)
- Saruta, M., Papadakis, K.A.: Capsule endoscopy in the evaluation and management of inflammatory bowel disease: a future perspective. *Expert Rev. Mol. Diagn.* **9**(1), 31–36 (2009)
- Carey, E.J., Leighton, J.A., Heigh, R.I., Shiff, A.D., Sharma, V.K., Post, J.K., Fleischer, D.E.: A single-center experience of 260 consecutive patients undergoing capsule endoscopy for obscure gastrointestinal bleeding. *Am. J. Gastroenterol.* **102**(1), 89–95 (2007)
- Wang, K., Wang, Z., Zhou, Y., Yan, G.: Squirm robot with full bellow skin for colonoscopy. In: Proceedings of the 2010 IEEE International Conference on Robotics and Biomimetics, pp. 53–57 (2010)
- Quaglia, C., Buselli, E., Webster, R.J., Valdastrì, P., Menciasci, A., Dario, P.: An endoscopic capsule robot: a meso-scale engineering case study. *J. Micromech. Microeng.* **19**(10), 11 (2009)
- Yang, W.A., Hu, C., Meng, M.Q.H., Dai, H.D., Chen, D.M.: A new 6D magnetic localization technique for wireless capsule endoscope based on a rectangle magnet. *Chin. J. Electron.* **19**(2), 360–364 (2010)
- Gao, M., Hu, C., Chen, Z., Zhang, H., Liu, S.: Design and fabrication of a magnetic propulsion system for self-propelled capsule endoscope. *IEEE Trans. Biomed. Eng.* **57**(12), 2891–2902 (2010)
- Wang, X., Meng, Q.H., Chen, X.: A locomotion mechanism with external magnetic guidance for active capsule endoscope. In: Engineering in Medicine and Biology Society (EMBC), 2010 Annual International Conference of the IEEE, pp. 4375–4378 (2010)
- Kim, B., Park, S., Park, J.O.: IEEE: Microrobots for a capsule endoscope. In: IEEE ASME International Conference on Advanced Intelligent Mechatronics, pp. 729–734 (2009)
- Hoeg, H.D., Slatkin, A.B., Burdick, J.W., Grundfest, W.S.: Biomechanical modeling of the small intestine as required for the design and operation of a robotic endoscope. In: Proceedings of IEEE International Conference on Robotics and Automation, pp. 1599–1606 (2000)
- Li, J., Huang, P., Luo, H.D.: Experimental study on friction of micro machines sliding in animal intestines. *Lubr. Eng.* **175**(3), 119–122 (2006)
- Baek, N.K., Sung, I.H., Kim, D.E.: Frictional resistance characteristics of a capsule inside the intestine for microendoscope design. *Proc. Inst. Mech. Eng. H* **218**(3), 193–201 (2004)
- Kim, J.S., Sung, I.H., Kim, Y.T., Kwon, E.Y., Kim, D.E., Jang, Y.H.: Experimental investigation of frictional and viscoelastic properties of intestine for microendoscope application. *Tribol. Lett.* **22**(2), 143–149 (2006)
- Kim, J.S., Sung, I.H., Kim, Y.T., Kim, D.E., Jang, Y.H.: Analytical model development for the prediction of the frictional resistance of a capsule endoscope inside an intestine. *Proc. Inst. Mech. Eng. H* **221**(H8), 837–845 (2007)
- Wang, X., Meng, M.Q.H.: An experimental study of resistant properties of the small intestine for an active capsule endoscope. *Proc. Inst. Mech. Eng. H* **224**(H1), 107–118 (2010)
- Wang, K.D., Yan, G.Z.: Research on measurement and modeling of the gastro intestine's frictional characteristics. *Meas. Sci. Technol.* **20**(1), 015803.1–015803.6 (2009)
- Li, H., Katsuhisa, F., Chernousko, F.L.: Motion generation of the capsuobot using internal force and static friction. In: 45th IEEE Conference on Decision and Control, pp. 6575–6580 (2006)
- Gregersen, H.: *Biomechanics of the Gastrointestinal Tract: New Perspectives in Motility Research and Diagnostics*, 1st edn. Springer, New York (2003)
- Tan, R., Liu, H., Su, G., Zhang, C., Li, H., Wang, Y.: Experimental investigation of the small intestine's viscoelasticity for the motion of capsule robot. In: IEEE International Conference on Mechatronics and Automation, ICMA 2011, pp. 249–253 (2011)
- Wu, J.H., Cheng, X.Y., Wei, Y.L., Zhou, Y.S., Zhu, Y.Q.: Rheological behavior of dog's small intestinal mucus. *J. Chongqing Univ (Natural Science Edition)* **23**(2), 10–12 (2000)
- Varum, F.J.O., Veiga, F., Sousa, J.S., Basit, A.W.: An investigation into the role of mucus thickness on mucoadhesion in the gastrointestinal tract of pig. *Eur. J. Pharm. Sci.* **40**(4), 335–341 (2010)
- Zhang, C., Su, G., Tan, R., Li, H.: Experimental investigation of the intestine's friction characteristic based on "internal force-static friction" capsuobot. In: IASTED International Conference on Biomedical Engineering, Biomed 2011, pp. 117–123 (2011)
- Ciarletta, P., Dario, P., Tendick, F., Micera, S.: Hyperelastic model of anisotropic fiber reinforcements within intestinal walls for applications in medical robotics. *Int. J. Robot. Res.* **28**(10), 1279–1288 (2009)